Superprotonic phase transition in mixed ammonium–caesium acid sulphate $Cs_{0.9}(NH_4)_{0.1}HSO_4$

T. Mhiri*, A. Daoud and M. Bouachir

Laboratoire de l'Etat Solide, Ecole Nationale d'Ingénieurs, 3038 Sfax (Tunisia)

F. Romain

Laboratoire de Spectrochimie IR et Raman, CNRS, 2 rue Henri Dunant, 94320 Thiais (France)

Abstract

Electrical conductivity, differential scanning calorimetry, X-ray diffraction, IR and Raman studies on $Cs_{0.9}(NH_4)_{0.1}HSO_4$ polycrystalline and single-crystal samples were carried out. A high temperature phase transition at 410 K to a superionic phase was found. A sudden jump (three orders of magnitude) in the conductivity plot confirms the presence of a transition at this temperature. The phase is characterized by a high electrical conductivity $(5 \times 10^{-3} \Omega^{-1} cm^{-1})$ and low activation energy $(E_a < 0.1 eV)$.

1. Introduction

Recently, the study of crystals of the hydrogen sulphate and selenate family $MHAO_4$ ($M \equiv Cs$, Rb, NH_4; $A \equiv S$, Se) has shown that the superionic phase transitions (SPTs) are due to disordering of the hydrogen bond system. This disorder consists of rotational motions of HAO_4^- anions and/or translational motion to a plastic and/or superionic state [1].

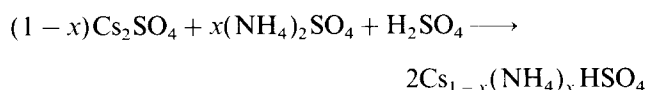The SPT can be described as "melting" of the $HS(Se)O_4^-$ conducting sublattice.

In previous work [2–4] we have shown that the controlled introduction of defects in the host framework allows the transition to be smoothed; the electrical properties in the high and low temperature phases are brought together and glass formation by quenching from the melt in $Cs_{1-x}M_xHSO_4$ ($M \equiv Li$, K, Rb) alloys is favoured.

In this paper we report and we discuss the results of structural investigations concerning a new mixed compound $Cs_{0.9}(NH_4)_{0.1}HSO_4$ obtained by differential scanning calorimetry (DSC), X-ray diffraction, and impedance and vibrational spectroscopy. They are used to obtain a better understanding of conductivity mechanisms.

2. Experimental details

Colourless and transparent single crystals of $Cs_{0.9}(NH_4)_{0.1}HSO_4$ were grown by slow evaporation at

---

*Author to whom correspondence should be addressed.

300 K of stoichiometric M_2SO_4–M'_2SO_4–H_2SO_4 (1 M) aqueous solutions [2]:

$$(1-x)Cs_2SO_4 + x(NH_4)_2SO_4 + H_2SO_4 \longrightarrow$$

$$2Cs_{1-x}(NH_4)_xHSO_4$$

Samples were characterized by their X-ray powder patterns. Caesium, nitrogen, sulphur and hydrogen contents were determined by chemical analysis (Service d'Analyse du CNRS, 69 Vernaison).

IR spectra of Nujol and Fluorolube mulls were examined on Perkin–Elmer 783 and 983 spectrophotometers in the 4000–200 cm^{-1} region.

Raman spectra of polycrystalline samples sealed in glass tubes were recorded on an RTI Dilor instrument using the 514.5 nm and 488.0 nm exciting lines of a Spectra-Physics argon ion laser.

Electrical impedances were measured in the 0.01 kHz–10 MHz range using a Hewlett–Packard 4192 A LF automatic bridge monitored by an Olivetti M24 microcomputer.

DSC was performed with a Perkin–Elmer DSC4 instrument between 100 and 500 K. Samples were wrapped in an aluminium gasket (not gas proof) and flushed with dry nitrogen.

3. Results and discussion

The crystal structure at room temperature was solved by Itoh *et al.* [5], and according to them $CsHSO_4$ is monoclinic, space group $P2_1/c$, $Z = 4$. Caesium hydrogen sulphate undergoes successive phase transitions

from a low temperature phase to an intermediate phase in the temperature range from 333 to 370.K on heating [6], and then to a superionic high temperature phase above 417 K, exhibiting an unusually high conductivity of about $10^{-2} \Omega^{-1} cm^{-1}$ [7]. In contrast, the crystal of the ammonium hydrogen sulphate exhibits pseudo-orthorhombic symmetry, space group $B2_1/a$, and its room temperature phase contains simultaneously cyclic dimers and infinite chains of hydrogen-bonded HSO_4^- anions [8] as in the case of $KHSO_4$. The NH_4HSO_4 crystal melts without reaching the superionic state [9–16]. For $RbHSO_4$, the superionic state can be induced by hydrostatic pressure [10]. On the contrary, NH_4HSO_4 undergoes a ferroelectric phase transition at $T < 270$ K [11].

3.1. Crystalline parameters and phase transitions

$Cs_{0.9}(NH_4)_{0.1}HSO_4$ single crystals were picked out of the mother liquor and cleaned with paper. After that samples were kept in a dry atmosphere. Typical sizes were 1.5 mm × 1 mm × 0.5 mm.

X-ray examination by rotating crystal, Weissenberg and precession methods reveals that the $Cs_{0.9}(NH_4)_{0.1}HSO_4$ crystal exhibits triclinic symmetry at room temperature with the following unit cell parameters:

$$a = 7.488(5) \text{ Å} \quad \alpha = 102.7°$$
$$b = 5.581(3) \text{ Å} \quad \beta = 98°$$
$$c = 3.642(4) \text{ Å} \quad \gamma = 116°$$

The X-ray powder patterns indicate that the structure of the mixed compound $Cs_{0.9}(NH_4)_{0.1}HSO_4$ is not similar to that of the $CsHSO_4$ compounds. The unit cell parameters in the triclinic phase allow us to index the powder diffractograms. The possible space group is either $P1$ or $P\bar{1}$.

The DSC method was used to find the phase transitions. Figure 1 shows typical DSC traces in the 100–
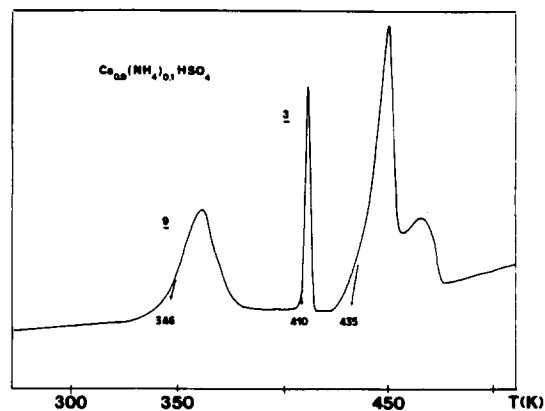
500 K temperature range for the $Cs_{0.9}(NH_4)_{0.1}HSO_4$ material. Two first-order phase transitions have been observed on heating and they are reversible. The first transition is observed at 346 K (phase I → phase II as in the case of $CsHSO_4$ observed at 338 K). The I → II transition has been interpreted in terms of the conversion of infinite chains $(HSO_4^-)_n$ into cyclic dimers $(HSO_4^-)_2$ [7]. Above 410 K there is a plastic superionic phase III characterized by substantial dynamic disorder (consisting of rapid HSO_4^- reorientations and fast H^+ diffusion) [4–13]. The superionic transition (initially observed at 417 K in $CsHSO_4$) is observed with a small temperature shift related to small structural changes. Phase transitions are thus spread out as a result of controlled defect introduction. The appearance of substantial structural disorder is evident from the peak broadening at the I → II transition. The $Cs_{0.9}(NH_4)_{0.1}HSO_4$ crystal starts to decompose at about 460 K; in the case of $CsHSO_4$ decomposition takes place at 480 K.

3.2. Electrical properties

Crystals and polycrystalline pieces were crushed and sintered at room temperature for a few hours under a 200 MPa stress. A mould evacuated by a vacuum pump was used. Dense translucent pellets (10 mm in diameter, 1–2 mm in thickness) were obtained. Silver paste electrodes were then deposited. Our measurements were performed at temperatures ranging from room temperature to 440 K.

Figure 2 shows conductivity–temperature $\log(\sigma T) = f(1/T)$ plots for the mixed compound $Cs_{0.9}(NH_4)_{0.1}HSO_4$. In this paper we discuss mainly the results obtained for the second heating (M_2) and the

Fig. 1. DSC traces of the $Cs_{0.9}(NH_4)_{0.1}HSO_4$ material. Heating rate, 10 K min^{-1} (ΔH (kcal mol^{-1}), enthalpy).
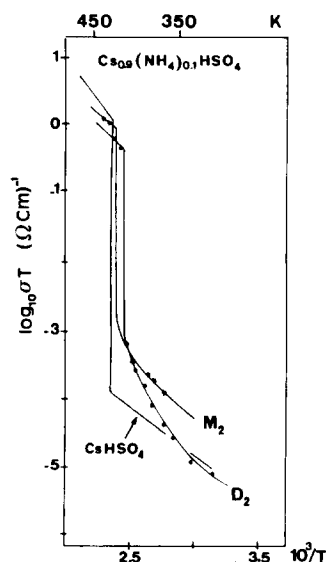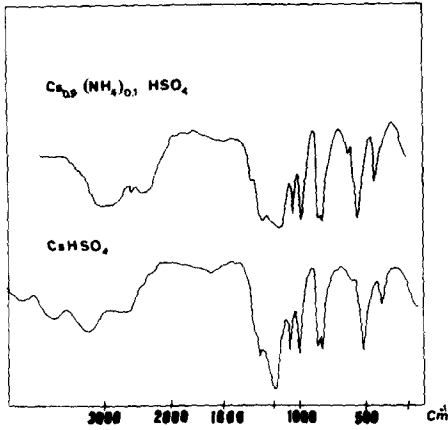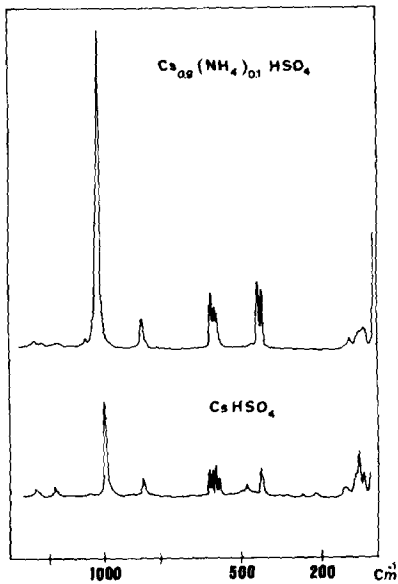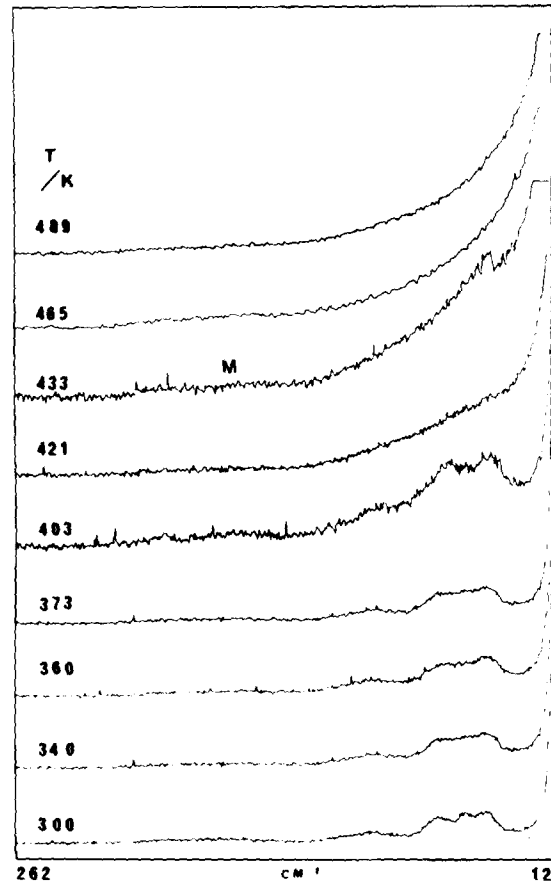

Fig. 2. Conductivity plots $\log_{10}(\sigma T) = f(1/T)$ for $CsHSO_4$ and $Cs_{0.9}(NH_4)_{0.1}HSO_4$ pellets. The second (M_2, D_2) heating (cooling) cycle is given.

Fig. 3. IR spectra of $Cs_{0.9}(NH_4)_{0.1}HSO_4$ and $CsHSO_4$ at 300 K.

Fig. 4. Raman spectra of $Cs_{0.9}(NH_4)_{0.1}HSO_4$ and $CsHSO_4$ at 300 K.

Fig. 5. Raman spectra in the range $12-262 \, cm^{-1}$ of $Cs_{0.9}(NH_4)_{0.1}HSO_4$ at various temperatures. The M spectra correspond to the molten state.

second cooling (D_2) runs. In the first run the conductivity can be increased by moisture traces at the sample surface. Conductivity plots exhibit a high conductivity jump (three orders of magnitude) at about 410 K and confirm the superionic transition already observed by DSC at the same temperature. Below the SPT temperature ($T = 410$ K), the conductivity is rather weak,

TABLE 1. Electrical properties of $Cs_{1-x}M_xHSO_4$ ($M^+ \equiv Li^+, Rb^+, NH_4^+$) materials

Compound	420 K		320 K		References
	σ $((\Omega \, cm)^{-1})$	E_a (eV)	σ $((\Omega \, cm)^{-1})$	E_a (eV)	
$CsHSO_4$	5×10^{-3}	0.20	10^{-7}	0.25	11, 13
NH_4HSO_4	10^{-3}	—	10^{-7}	0.33	9
Li					
$Cs_{0.9}Li_{0.1}HSO_4$	10^{-3}	0.15	5×10^{-6}	0.15	3
Rb					
$Cs_{0.9}Rb_{0.1}HSO_4$	5×10^{-3}	0.05	10^{-7}	0.20	3
Ammonium					
$Cs_{0.9}(NH_4)_{0.1}HSO_4$	5×10^{-3}	0.05 ± 0.01	10^{-6}	0.08 ± 0.02	This work

TABLE 2. Raman frequencies of $Cs_{0.9}(NH_4)_{0.1}HSO_4$ for different phases between 10 and 1310 cm^{-1}

Phase I: 300 K	Phase II		Phase III: 421 K	Molten state	Assignment
	360 K	373 K			
			1240 vw	1240	$v(S-O)$
			1180 vw	1180	
1070 vw	1066 w	1066 w			
				1034 vs, vb	
			1030 vs, b		
1020 vs	1020 vs	1020 vs			
805 s	810 s	810 s	825 s, vb	830 s, vb	$v(S-OH)$
600 s	596 s	596 s			$v_4(SO_4)$
590 s	586 s	585 s	586 s, b	586 s, b	
580 m	577 sh	578 sh			
425 s	426 s	426 s			$v_2(SO_4)$
415 s	416 s			418 s, b	
			413 s, b		
		394 s			
165 w					$T'-R'(HSO_4^-)$
	155 w	155 w	155 w, b	150 w, b	
95 w	95 w	93 m			
65 m		65 m			$T'(Cs^+)$
	60 m				
55 m					
45 m	43 m	44 m			
			R	R	

v, T', R', stretching, translational and rotational vibration respectively; s, strong; m, medium; w, weak; v, very; b, broad; sh, shoulder; R, Rayleigh wing.

$10^{-6} \Omega^{-1} cm^{-1}$ (M_2) and $10^{-7} \Omega^{-1} cm^{-1}$ (D_2) at 325 K, with a low activation energy value of the order of 0.08 eV (M_2).

In the low temperature phase, the conductivity increases on heating but its temperature dependence cannot be described by an Arrhenius law. This behaviour is often observed for superionic materials containing a high proportion of static defects (structure defects such as $S_2O_7^{2-}$ and SO_4^{2-}) hindering the dynamic disorder [14]. In the high temperature phase at $T = 420$ K the value of the electrical conductivity reaches $5 \times 10^{-3} \Omega^{-1} cm^{-1}$ (superionic conductor phase) and the value of the activation energy is about 0.05 eV.

We deduce that partial substitution of caesium (Cs^+) ions by ammonium (NH_4^+) ions leads to a lowering of the activation energy from 0.25–0.30 eV in the case of pure $CsHSO_4$ to a value lower than 0.1 eV in the case of the mixed compound $Cs_{0.9}(NH_4)_{0.1}HSO_4$ as observed with $Cs_{1-x}Li_xHSO_4$ alloys [12]. Conductivity values σ and activation energies E_a in the high temperature (420 K) and the low temperature (323 K) regimes are given in Table 1 for comparison between

$CsHSO_4$, NH_4HSO_4 and the mixed compounds $Cs_{0.9}(NH_4)_{0.1}HSO_4$.

3.3. Structural modifications

IR and Raman spectroscopies can help to provide an idea of the modification of the crystalline structure with respect to that of pure $CsHSO_4$. Analysis of the S–O and S–OH stretching region is a good tool to study the change in the HSO_4^- association and in the hydrogen bonding [15].

Figures 3 and 4 and Table 2 show typical IR and Raman spectra of the mixed compound $Cs_{0.9}(NH_4)_{0.1}HSO_4$ and give frequencies. These vibrational spectra are similar to those of $CsHSO_4$ except for the presence of new IR bands due to the stretching of NH_4^+: $v_1 = 3075$ cm^{-1}, $v_2 = 1400$ cm^{-1}, $v_3 = 3150$ cm^{-1} and $v_4 = 1675$ cm^{-1}. However, most information can be obtained from S–O and S–OH stretching modes near 1025 cm^{-1} and 860 cm^{-1} respectively, indicating the presence of some cyclic dimers ($\Delta v = v_{S-O} - v_{S-OH} = 165$ cm^{-1}), and from the low frequency Raman spectra as in $Cs_{1-x}M_xHSO_4$ solid solutions [2].
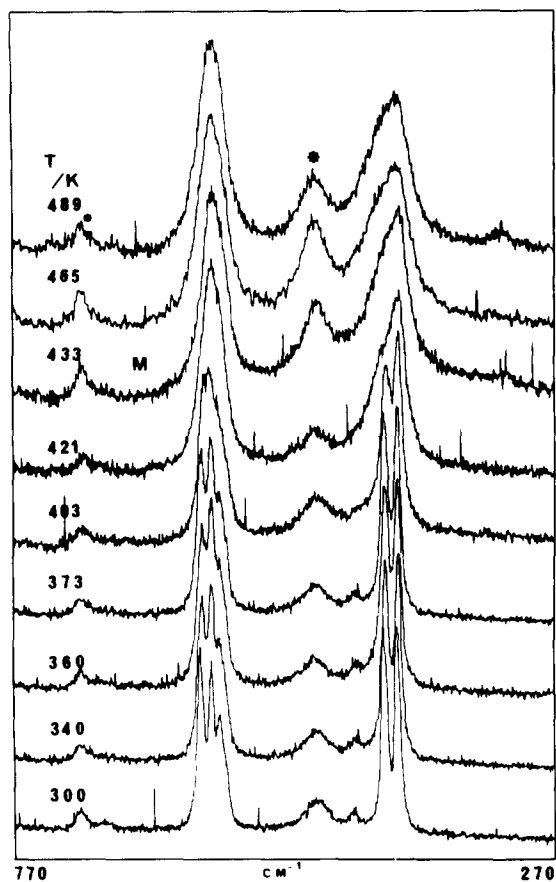
Fig. 6. Raman spectra between 270 and 770 cm^{-1} of different phases in $Cs_{0.9}(NH_4)_{0.1}HSO_4$: *, oil bands of the heating cell.

Fig. 7. Raman spectra between 730 and 930 cm^{-1} of $Cs_{0.9}(NH_4)_{0.1}HSO_4$ at various temperatures.

In the external modes we observe changes in the low frequency Raman spectra: in the case of $Cs_{0.9}(NH_4)_{0.1}HSO_4$ disorder is evidenced by the broadening of the $T'(Cs^+)$ modes near 45, 60 and 85 cm^{-1}. The $T'(NH_4^+)$ and $R'(NH_4^+)$ modes at about 180 cm^{-1} and 250 cm^{-1} respectively do not appear on account of the low rate substitution of NH_4^+ ions. Introduction of cationic defects in $Cs_{1-x}(NH_4)_x HSO_4$ with high ammonium content will be very interesting because ammonium contributes to the increase in the dynamic and static disorder and phase transitions are thus spread out. The properties of $Cs_{1-x}(NH_4)_x HSO_4$ ($0 < x < 1$) alloys as a function of ammonium content are under study.

3.3.1. Phase transitions

Raman spectra of $Cs_{0.9}(NH_4)_{0.1}HSO_4$ between 10 and 1310 cm^{-1} at different temperatures are shown in Figs. 5–8. They are different and allow us to characterize the three phases (I, II and III) unambiguously.

The low and middle frequency spectrum (10–1310 cm^{-1}) of $Cs_{0.9}(NH_4)_{0.1}HSO_4$ appears to be sensi-
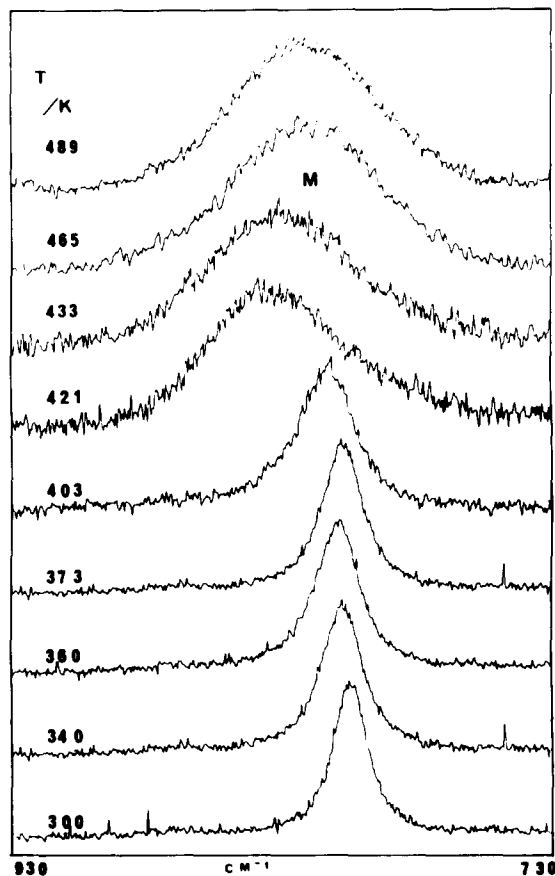
tive to temperature. Two features are noticeable at 340 K (phase II) and at 405 K (phase III). Phase II at 340 K is characterized by a slight increase in broadening of the bands, showing that disordering of HSO_4^- ions takes place.

The appearance of a substantial disorder above the SPT at 405 K is evident from the band broadening (Table 2, Figs. 7 and 8) and the large increase in the Rayleigh wing. The Rayleigh wing becomes smooth as expected for a liquid. This indicates that the orientational disorder of HSO_4^- species takes place at the superionic transition. Figures 7 and 8 show the frequency and width of the $v(S-OH)$ and $v(S-O)$ Raman bands as a function of temperature.

The Raman spectra recorded at 433 K correspond to the molten state (M). The modification is not as drastic when melting takes place: the broadness of the band increases slightly and the bands become more symmetrical.

Thus, Raman study confirms the phase transitions previously evidenced by DSC.
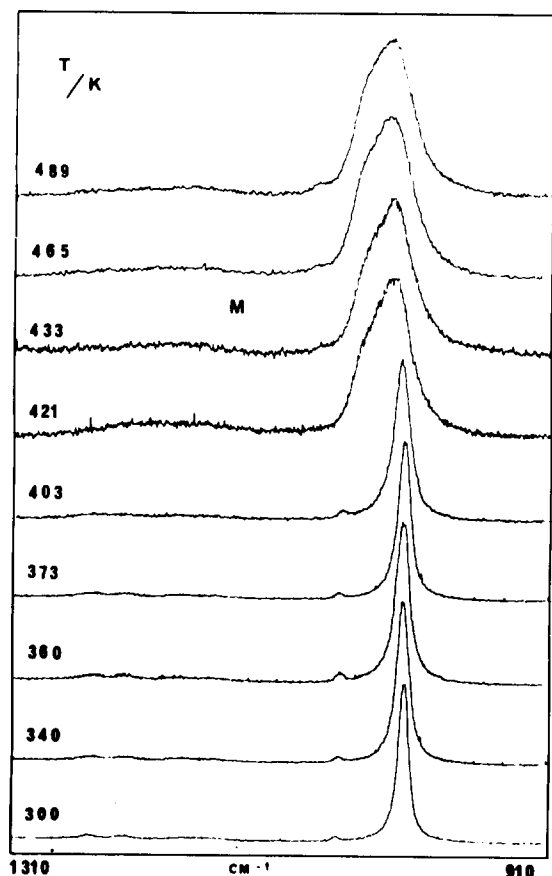
Fig. 8. Raman spectra in the range 910–1310 cm⁻¹ of $Cs_{0.9}(NH_4)_{0.1}HSO_4$ at various temperatures.

4. Conclusion

The mixed compound $Cs_{0.9}(NH_4)_{0.1}HSO_4$ exhibits two first-order phase transitions. These transitions are of order–disorder type. The first at about 346 K (I → II) involves not only more orientational disorder but also a partial conversion of infinite chains $(HSO_4^-)_n$ to cyclic dimers $(HSO_4^-)_2$ as observed in mixed alkali acid sulphates $Cs_{1-x}M_xHSO_4$ (M ≡ Li, K, Rb) [2–4].

Finally, the II → III transition at 410 K is an SPT leading to a highly disordered plastic phase. The superionic transition corresponds to the melting of the proton sublattice to a "quasi-liquid" state where proton and SO_4^{2-} ion disorder contributes to the unusually high conductivity as in the case of $CsHSO_4$ and its derivative mixed compounds $Cs_{1-x}M_xHSO_4$.

References

1 Ph. Colomban and A. Novak, J. Mol. Struct., 177 (1988) 277.
2 T. Mhiri, A. Daoud and Ph. Colomban, Phase Transit., 14 (1989) 233.
3 T. Mhiri and Ph. Colomban, Solid State Ionics, 35 (1989) 99.
4 T. Mhiri, A. Daoud and Ph. Colomban, Solid State Ionics, 44 (1991).
5 K. Itoh, T. Ukeda, T. Ozaki and E. Nakamura, Acta Crystallogr. C, 46 (1990) 358.
6 A. V. Belushkin, I. Natkaniec, N. M. Pakida, L. Shuvalov and J. Wasicki, J. Phys. C, 20 (1987) 671.
7 Ph. Colomban, M. Pham-Thi and A. Novak, Solid State Ionics, 24 (1987) 193.
8 R. Pepinsky and K. Vedam, Phys. Rev., 117 (1960) 1502.
9 A. I. Baranov, R. M. Fedosyuk, M. M. Schagina and L. A. Shuvalov, Ferroelectr. Lett., 2 (1984) 25.
10 R. Pepinsky and K. Vedam, S. Hoshino and Y. Okaya, Phys. Rev., 111 (1958) 1508.
11 A. I. Baranov, L. A. Shuvalov and N. M. Schagina, JETP Lett., 36 (1982) 459.
12 T. Mhiri, Thèse d'Etat, Tunis, 1991.
13 N. G. Hainovskiy and E. Hairetdinov, Izv. Sib. Ot. SSSR, Ser. Khim. Nauk, 8 (1985) 33.
14 Ph. Colomban, Solid State Ionics, 21 (1986) 97.
15 Ph. Colomban, M. Pham-Thi and A. Novak, J. Mol. Struct., 161 (1987) 1.
16 A. I. Baranov, E. G. Ponyatovskii, V. V. Sinitsyn, R. M. Fedosyuk and L. A. Shuvalov, Kristallografiya, 30 (1985) 1121.